Design of an RFID-Based Battery-Free Programmable Sensing Platform

5 authors, including:

Some of the authors of this publication are also working on these related projects:

NFC-WISP View project

WISP Localization View project

Design of an RFID-Based Battery-Free Programmable Sensing Platform

Alanson P. Sample, *Student Member, IEEE*, Daniel J. Yeager, *Student Member, IEEE*, Pauline S. Powledge, Alexander V. Mamishev, *Senior Member, IEEE*, and Joshua R. Smith, *Member, IEEE*

Abstract—This paper presents the Wireless Identification and Sensing Platform (WISP), which is a programmable battery-free sensing and computational platform designed to explore sensor-enhanced radio frequency identification (RFID) applications. WISP uses a 16-bit ultralow-power microcontroller to perform sensing and computation while exclusively operating from harvested RF energy. Sensors that have successfully been integrated into the WISP platform to date include temperature, ambient light, rectified voltage, and orientation. The microcontroller encodes measurements into an Electronic Product Code (EPC) Class 1 Generation 1 compliant ID and dynamically computes the required 16-bit cyclical redundancy checking (CRC). Finally, WISP emulates the EPC protocol to communicate the ID to the RFID reader. To the authors' knowledge, WISP is the first fully programmable computing platform that can operate using power transmitted from a long-range (UHF) RFID reader and communicate arbitrary multibit data in a single response packet.

Index Terms—Programmable radio frequency identification (RFID), RFID sensors, sensor, transponder, UHF, wireless power.

I. INTRODUCTION

RADIO FREQUENCY identification (RFID) systems typically consist of small low-cost battery-free devices, called tags, which use the radio signal from a specialized RFID reader for power and communication. When queried, each tag responds to a unique identification number by reflecting energy back to the reader through backscatter modulation. Tags are often application-specific fixed-function devices that have a range of 10–50 cm for inductively coupled devices and 3–10 m for UHF tags. Traditionally, RFID tags have been used as a replacement for barcodes in such applications as supply chain monitoring, asset management, and building security [1].

Industrial efforts in the development of RFID technology have produced a robust physical layer capable of wirelessly powering and querying a tag. This core technology enables a new class of wireless battery-free devices with communication, sensing, computation, and data storage capabilities. Unconstrained by batteries, these devices have the potential to operate for years if not decades.

The authors in [2] present network architectures for an RFID-enhanced environment, where objects are seamlessly tracked and monitored. The implementation of an environment augmented with RFID to enhance the quality of life and independence of elderly citizens is discussed in [3]. In this example, participants wear small RFID reader bracelets that report interaction with tagged objects. Activities can be inferred from these data and reported to caregivers. Specific applications for sensor-enhanced RFID tags are identified in [4] and include infrastructure and object monitoring, automatic product tamper detection, identification of harmful agents, and biomedical devices for noninvasive monitoring.

Conventional RFID applications are also benefiting from sensor-enhanced RFID tags. A commercially available RFID tag for detecting dangerous temperatures in food products during transit is reported in [4]. This product suggests the possibility that although the price of RFID tags may not sufficiently decrease for all potential applications, sensor-enhanced tags may provide a substantial increase in functionality for the same price as conventional RFID tags.

To date, there are several approaches for incorporating sensing capabilities into RFID. Active tags, which are a subclass of RFID tags, use batteries to power their communication circuitry, sensors, and microcontroller. Active tags benefit from relatively long wireless range (approximately 30 m) and can achieve high data and sensor activity rates. However, the batteries required by active tags are disadvantageous for device cost, lifetime, weight, and volume.

In contrast, passive sensor tags receive all of their operating power from an RFID reader and are not limited by battery life. There are several examples of application-specific nonprogrammable passive tags with integrated temperature and light sensors, as well as an analog-to-digital converter (ADC) [5], [6]. One attractive feature of passive sensor tags is the prospect of permanently embedding them in objects for structural, medical, or product monitoring. Another advantage is their suitability for applications in which neither batteries nor wired connections are feasible, for weight, volume, cost, or other reasons. A limitation of purely passive sensor tags is the requirement of proximity to an RFID reader. However, other methods such as solar, thermal, or kinetic energy harvesting could be used as a secondary power source if needed.

A further consideration is the configurability and computational power of RFID sensor tags. Existing devices are
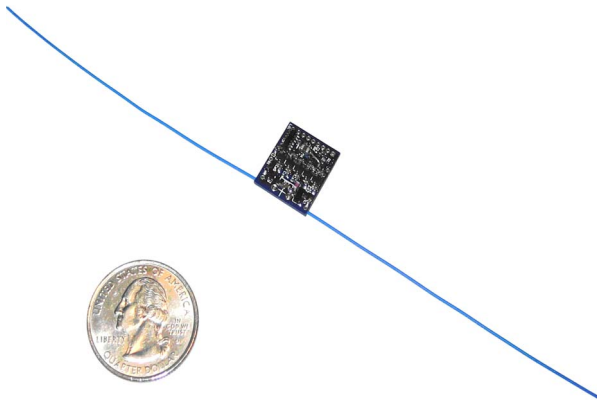
Fig. 1. WISP platform.

generally fixed function with respect to sensory inputs, and they lack computational capabilities. A commercially available RFID tag with some additional functionality is described in [7]; however, this device can only transmit 1 bit of sensor data in addition to its ID. Furthermore, it is limited by a short read range due to its 125-kHz operating frequency.

This paper presents the design and performance of the Wireless Identification and Sensing Platform (WISP), which is a battery-free programmable RFID sensor device (Fig. 1). Compliant with the Electronic Product Code (EPC) Class 1 Generation 1 protocol, WISP can transmit 64 bits of data per query and is fully configurable due to its ultralow-power 16-bit general-purpose microcontroller. Similar to conventional passive UHF RFID tags, WISP has no batteries and is completely powered via the RF energy transmitted by an RFID reader.

The architecture of WISP allows the measurement of virtually any low-power sensor, which is also wirelessly powered by the RFID reader. WISP is implemented as a printed circuit board (PCB), which offers a flexible platform for exploring new sensor integration schemes and applications. To the authors' knowledge, WISP represents the first microcontroller to be integrated as part of a passive UHF RFID tag, with an operating range of several meters.

The general-purpose WISP described in this paper was preceded by several less-capable devices (also called WISPs) that were described in earlier publications by our group. α-WISP [8] used two mercury switches to mechanically toggle between two commercially produced RFID integrated circuits (ICs). π-WISP [9] used a microcontroller powered by harvested RF power to activate a GaAs RF switch, which multiplexed two commercially available RFID ICs to one tag antenna. This device could transmit at most 1 bit of sensor data per query and used two separate antennas for communication and power harvesting. The significant difference between the previous work and the WISP presented in this paper is that the microcontroller is now implementing the EPC protocol, and no commercial RFID ICs are used in the design. This gives WISP the ability to control all 64 bits of the ID for data encoding versus one effective bit for the previous approaches based on enabling and disabling commercial tag ICs. Furthermore, the device described in this paper uses a single antenna for power harvesting and communication, whereas the approach in [9] required separate antennas for these two functions.

This paper presents detailed discussion of the WISP design, power budget, and bidirectional communication capabilities. The architecture and algorithms of WISP are presented in Sections II and III. Next, a detailed power budget analysis shows the wireless range and sensor load capabilities of WISP in Section IV. Finally, the experimental results and sensor applications are shown in Sections V and VI.

II. WISP ARCHITECTURE

The development of WISP using a PCB design departs from conventional RFID design as an IC. The primary advantages of PCB implementation over IC are the fast design iteration time, low development cost, and modularity; it is easy to add or remove sensors (produced on heterogeneous processes) to the basic WISP platform, as required by the application. In contrast, IC implementations can include custom components, typically consume less power than discrete PCB designs, and yield a smaller form factor device. Also, integrating sensors into RFID ICs may present process integration and packaging challenges.

A block diagram of WISP is shown in Fig. 2. An antenna and an impedance-matching circuit precede the analog front end. The power harvester block rectifies the incoming RF energy into dc voltage to power the system. The demodulator follows the envelope of the RF carrier wave to extract the amplitude-shift-keyed (ASK) data stream. This extracted baseband waveform is read by the MSP430 microcontroller (MCU) to receive downlink data from the reader. Uplink data are sent via the modulator circuit, which functions by changing the antenna impedance. Finally, onboard sensors are powered and measured by the MCU.

The WISP platform depicted in Fig. 1 is made of a four-layer FR4 PCB with components on both sides. A dipole antenna made of 22-gauge (0.6-mm-diameter) copper magnet wire is visible. The WISP in its base configuration has two onboard sensors, i.e., a circuit for measuring the rectified supply voltage and a temperature sensor. Small header pins expose all ports of the microcontroller for expansion to daughter boards, external sensors, and peripherals.

A. Analog Front End

A schematic of the WISP analog circuitry is shown in Fig. 3. The WISP analog front end slightly differs in purpose from that of conventional RFID tags. Due to the relatively high power consumption of WISP, the rectifier is designed to supply more current than ordinary tags. This circuit is excited by commercial EPC Class 1 Generation 1 compliant readers operating at 902–928 MHz with an allowable transmission power of 4 W_{EIRP} (effective isotropic radiated power).

Due to loss in signal strength over transmission distance (path loss), there is potentially very little power available for the tag. Therefore, efficient conversion of the incoming RF energy to dc power for the tag is an important design consideration. A matching network provides maximum power transfer from the antenna to the rectifier, and a five-stage voltage-doubling circuit converts the incoming power to voltage. Low-threshold RF Schottky diodes are used to maximize the voltage output of the rectifier. Finally, this rectified dc voltage is stored in
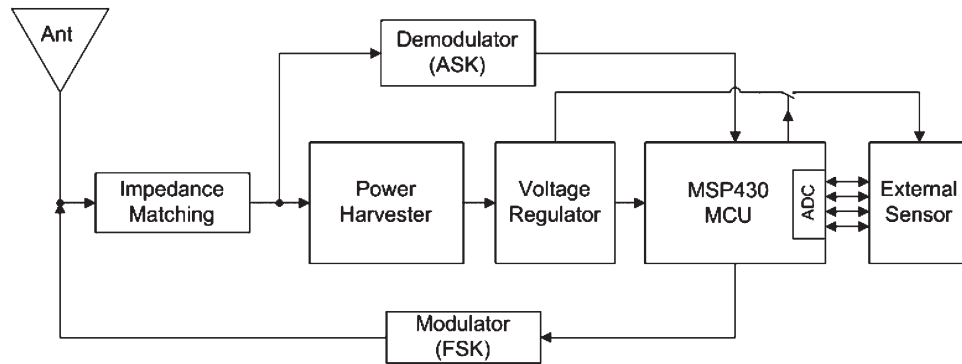
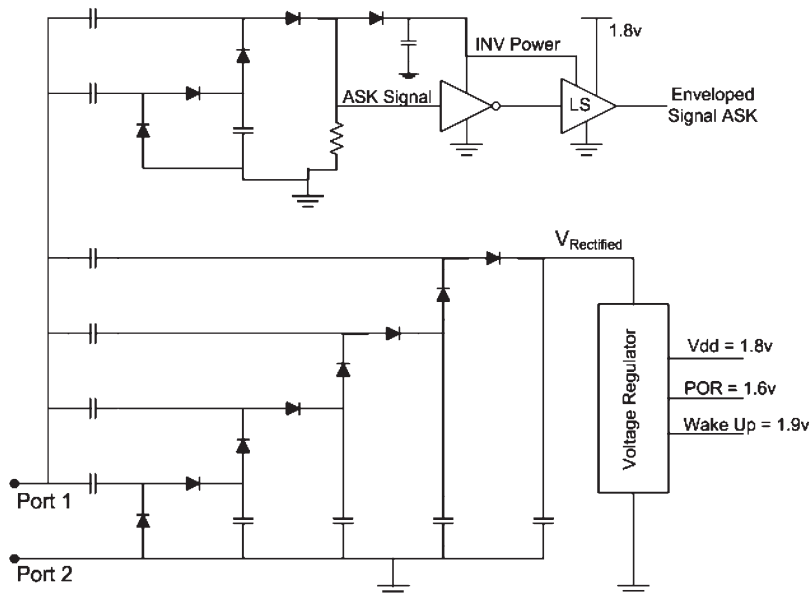Fig. 2.   Block diagram of the WISP platform.

Fig. 3.   Schematic of (bottom) WISP power harvesting and (top) ASK demodulation circuit.

a large capacitor and supplied to a 1.8-V regulator to power the WISP.

The WISP's discrete matching network, which is composed of a series inductor and parallel trimmable capacitor, was tuned until the output voltage of the WISP was maximized. Note that the power harvester is a nonlinear device, and its efficiency is load dependent. Ultimately, the front end must be tuned to provide maximum output voltage in the presence of the desired load.

B. Demodulation and Modulation

To encode reader-to-tag data, the reader amplitude modulates the 915-MHz RF carrier wave it emits. Normally, the carrier waveform remains at a constant amplitude; when bits are transmitted, the amplitude of the carrier drops to approximately 10% of its normal value. The duration of the "break" indicates a logical "one" or a "zero." To decode these data, the RF signal is fed through a two-stage voltage-doubling rectifier in parallel with the main harvester. This "mini-harvester" appears at the top of the schematic. The first two voltage-doubling stages of the mini-harvester, in conjunction with the resistor

and capacitor, effectively demodulate the 915-MHz carrier and leave a baseband data signal on the order of 70 kHz. The final "extra" diode (the top rightmost in the schematic) performs an additional rectification step, removing the 70-kHz data signal and leaving a slowly varying average power level that provides a dynamic reference for bit detection. The 70-kHz data signal is fed through a Schmitt trigger inverter and level shifter to convert the relative magnitude of the incoming data waveform into a 1.8-V logic level for the MSP430.

RFID tags do not actively transmit radio signals. Instead, they modulate the impedance of their antenna, which causes a change in the amount of energy reflected back to the reader. This modulated reflection is typically called backscatter radiation. To change the impedance of the antenna, a transistor is placed between the two branches of the dipole antenna. When the transistor conducts current, it short circuits the two branches of the antenna, changing the antenna impedance; in the nonconducting state, the transistor has no effect on the antenna, and thus, the power harvesting and data downlink functions occur as if it were not present. This impedance modulation is currently implemented with a 5-GHz RF bipolar junction transistor that allows for effective shunting of the 915-MHz carrier wave.

C. Digital Section and Power Conditioning

As the power available to RFID tags is extremely limited, careful component selection must be made to minimize current consumption. As advances in IC manufacturing now allow discrete components with less than 1-μA current consumption and 1.8-V operation, it is now possible to construct working wirelessly powered RFID tags with discrete components.

The general-purpose computation capabilities of WISP are provided by an ultralow-power microcontroller. This 16-bit flash microcontroller, i.e., the MSP430F1232, can run at up to 4 MHz with 1.8-V supply voltage and consumes approximately 600 μA when active for this choice of frequency and voltage. Of particular interest for low-power RFID applications, the MSP430 has various low-power modes. Its minimum RAM retention supply current is only 0.1 μA at 1.5 V. The device provides over 8 kB of flash memory, 256 B of RAM, and a 10-bit 200 kilosample-per-second ADC. The low-power consumption of this relatively new device is a critical factor in enabling use of a general-purpose microcontroller in passive RFID systems.

Another critical design consideration is operation with uncertain power supply conditions. Because the available RF power greatly varies throughout device operation, a supervisory circuitry is necessary to wake and sleep the device based on the supply voltage level. WISP uses a 1.9-V supervisor and a 1.6-V power-on-reset to control the device state and reset the microcontroller, respectively. The supervisor provides roughly 100 mV of headroom on the storage capacitor above the 1.8-V regulator voltage. This serves to buffer the supply voltage from dropping below 1.8 V due to the large power consumption of the microcontroller in active mode. This is further discussed in Section IV.

III. SOFTWARE

The onboard MSP430 programmable microcontroller is responsible for taking sensor measurements, embedding sensor or other data into an EPC-complaint ID, and implementing EPC Class 1 Generation 1 communication between the WISP and an RFID reader. Unlike active (battery-powered) tags, an energy-efficient microcontroller firmware is essential to maximize the wireless range of WISP. WISP also greatly varies from configurable silicon tag implementations; a user-defined firmware allows WISP to perform arbitrary computation, data filtering, and sensor measurements. The WISP software can be described on three levels. At the lowest level is the communication code, which enables bidirectional communication by sampling downlink data bits and generating uplink data bits. The next level, i.e., state and power management, is responsible for managing the device state, including sleep versus active modes. The third level implements the application layer protocol for encoding sensor data in the tag ID. This application layer is driven by a user application on a computer, which controls the RFID reader and decodes sensor data from IDs that are reported by the reader.

A. Packet Decoding and Encoding

A considerable challenge when programming the MSP430 involves meeting the timing constraints of the EPC protocol

while still maintaining a low clock frequency. RFID tags that have custom state machines are designed at the hardware level to receive and send using the EPC protocol. The general-purpose MSP430 must be carefully tuned to perform EPC communication both in the reception and transmission of data. In particular, a mix of C and assembly language is used, where the C code maintains ease of configurability for the firmware for different sensor applications, and the assembly code allows fine-grained control of the timing of the MSP430 for EPC communication.

The EPC protocol employs ASK modulation to encode data to the tag, representing the data bits 1 and 0 with long and short gaps in RF power, respectively. To receive data from the reader, the MSP430 uses the periodic edge of the waveform as a hardware interrupt and then, during the interrupt service routine, resamples the bit line to detect a 1 or 0 during the differentiated part of the waveform. These data are quickly shifted into memory before repeating this process. To detect the end of transmission, a timer is refreshed during each bit. When bits are no longer received, the timer expires, the packet is interpreted, and, if appropriate, a response is sent to the reader.

B. System State and Power Management Algorithm

Meeting the low-power requirements of passive RFID tags requires that the MCU dissipates, on average, as little power as possible. Fig. 4 shows the operational power cycle of the microprocessor. The system is event driven by external interrupts from either the voltage supervisor signal or the bit line communication interrupt. As shown in the diagram, the microcontroller sleeps between events to conserve power.

There are two active mode blocks. The first, which is designated as "Generate Packet," powers and samples an attached sensor and calculates cyclical redundancy checking (CRC) to complete the EPC-compliant ID. Next, the firmware waits for an RFID query, which triggers the second active block called "Receive and Transmit." The microcontroller receives the reader command and responds with the generated ID if the query is recognized. While not shown in Fig. 4, the same receive-and-transmit sequence is typically repeated twice to increase communication reliability.

C. Sensor Data Encoding

To communicate sensor data from WISP to a computer through an RFID reader, the data are encoded into the tag ID. Using the first byte after the CRC to denote the type of sensor attached, the remaining seven bytes are then used to encode sensor data. The onboard ADC measures with 10-bit accuracy, allowing a maximum of five measurements per tag ID. These data are parsed by a computer in real time to display the most recent measurements reported by WISP.

IV. POWER BUDGET

One of the significant challenges of incorporating microcontrollers, sensors, and peripherals into passive RFID technology is the ability to manage the large power consumption of these
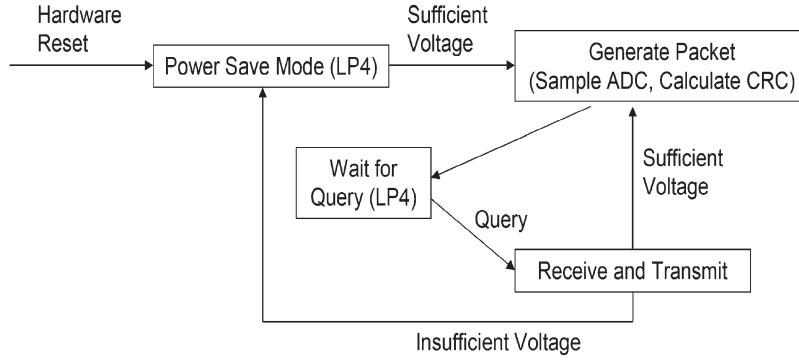
Fig. 4.   Operational power cycle.

devices. For example, the MSP430F1232 running at 3 MHz consumes approximately 470 μA at 1.8 V. The resulting power consumption is significantly larger than typical passive RFID tags. Under these conditions, the harvester cannot continuously supply power to the WISP during a single reader query.

One method to overcome this challenge is to use a large storage capacitor (on the order of 10 μF) to accumulate charge over multiple EPC queries. Once sufficient voltage is obtained, the WISP can operate in burst mode, polling sensors and communicating with the RFID reader. This approach of duty cycling is often used in low-power applications; however, this presents a challenge for RFID networks when WISP is not necessarily able to respond to each reader query.

The next section examines the issues related to powering the WISP from three perspectives. First is the received RF power required to turn on the device, the second is the operating duty cycle based on input power, and the last is the energy needed in the storage capacitor for active operation of the microcontroller and additional sensors.

A. Turn-On Power Requirement

In the presence of the RFID reader, the WISP's RF rectifier will charge the storage capacitor until the power input to the device equals the power lost due to quiescent current, i.e.,

$$P_{\text{in}} = P_{\text{loss}} \equiv V_{\text{rectified}} \times I_{\text{loss}}. \tag{1}$$

Thus, a key parameter for maximizing the read distance of WISP is minimizing the quiescent current consumption so that the minimum turn-on voltage of 1.9 V (supervisor threshold) can be rectified with the lowest possible input power. To characterize the system, a network analyzer was used to inject a continuous 915-MHz waveform into the antenna ports of the WISP. Fig. 5 shows the resulting plot of rectified voltage versus input power when WISP is in sleep mode. Using the minimum input power needed for activation from Fig. 5, the expected operating distance for WISP can be calculated with the following logarithmic form of the Friis equation for path loss, with a term for polarization loss included:

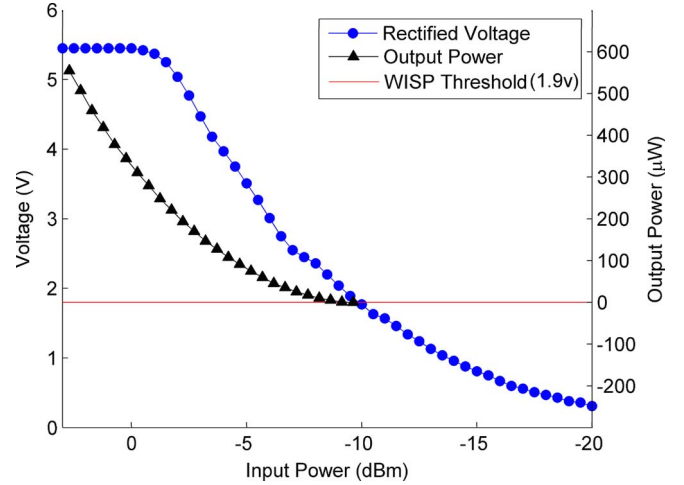$$P_R = P_T - 20\log\left(\frac{4\pi d}{\lambda}\right) + G_T + G_R - L_P. \tag{2}$$

Fig. 5.   (Left scale) Rectified voltage and (right scale) output power at 1.9 V versus input power measurements using a network analyzer for RF signal insertion into the antenna ports. The rectified voltage was measured with the WISP in sleep mode (only quiescent current draw). The output power was measured at an output voltage of 1.9 V, set by a power supply, and measured by an ammeter. The output power drops to zero when the harvester voltage reaches 1.9 V, because in this condition, the harvester drives zero current into the power supply.

The transmit power of the reader is $P_T = 1$ W $= 30$ dBm. Its center frequency is 915 MHz, corresponding to wavelength $\lambda = 0.33$ m. The transmit antenna gain is $G_T = 6$ dBi [this yields an EIRP of 4 W_{EIRP}, which is the United States regulatory limit for this Industrial, Scientific, and Medical (ISM) band]. The receive antenna gain is $G_R = 2$ dBi (the standard gain figure for a dipole antenna), and the polarization loss is $L_P = 3$ dB. Loss L_P occurs because only half of the power transmitted from the circularly polarized transmit antenna is received by the linearly polarized receive dipole antenna. Using the operating thresholds of -9.5 dBm from Fig. 6, (2) predicts a maximum operational range of 4.3 m.

B. Duty Cycle

While a rectified voltage (rather than power) determines the maximum achievable range, the operational duty cycle (percentage of the time WISP can be active) is determined by the amount of rectified power. In practice, the rectified voltage will typically remain near the threshold voltage (1.9 V). This
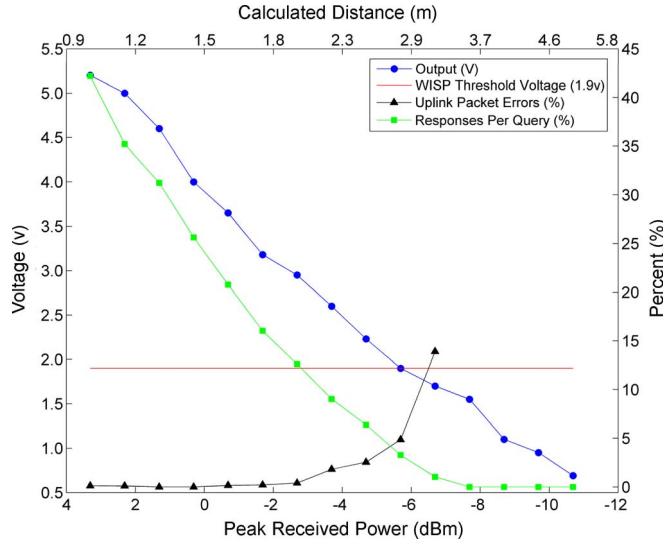
Fig. 6. WISP performance. Harvested voltage, uplink packet errors, and *Responses per Query* as a function of input power. The horizontal line with no markers shows the WISP operating voltage threshold of 1.9 V. The line marked with diamonds shows the harvested voltage. WISP cannot operate when the harvested voltage is less than the operating threshold voltage. The uplink packet error is the number of failed uplink packets divided by attempted uplink packets, expressed as a percentage. *Responses per Query* is the percentage of issued reader queries that return a packet with a valid CRC.

is due to the operation of the supervisor, which transitions the WISP from sleep to active mode, resulting in the consumption power whenever the stored voltage exceeds this operating point. Therefore, it is important to characterize the output power of the harvester at 1.9 V. This is accomplished by fixing the output voltage at 1.9 V using a power supply and measuring the amount of current that is supplied by WISP. Then, the duty cycle of WISP (percentage of the time in active mode) is estimated as the ratio of rectifier output power to WISP active power consumption, i.e.,

$$\frac{P_{\text{out}}}{P_{\text{active}}} = \frac{T_{\text{on}}}{T_{\text{on}} + T_{\text{sleep}}} = \text{Duty cycle.} \quad (3)$$

In this equation, P_{out} is the output power of WISP, P_{active} is the active power consumption, T_{on} is the time in active mode, and T_{sleep} is the time in sleep mode. For example, the power rectified at 0 dBm (310 μW) divided by the active power consumption (1.8 V $*$ 600 μA = 1.12 mW) yields a duty cycle of 27%. This agrees well with the experimental values, which are presented in Section V.

C. Active Energy Consumption

Since the rectifier cannot supply enough power for continuous operation, it is important to quantify the amount of energy that needs to be stored to power WISP during active periods. During one EPC Gen 1 communication cycle, the complete WISP (not just the microcontroller) consumes, on average, 600 μA $*$ 1.8 V = 1.08 mW. A single query takes 2 ms, including reader and tag communication. Using the expression for the energy stored in a capacitor ($1/2\, CV^2$, with $C = 10\ \mu$F), the amount of voltage headroom needed above 1.8 V is 116 mV,

resulting in a total minimum voltage threshold of 1.91 V for a complete packet transmission.

The same method for calculating the required stored energy can be used when selecting sensors for the WISP platform. Sensor tasks and packet generation are generally done prior to the EPC query. However, it is reasonable to assume that when performing sensor applications, the MCU will exhibit a similar current consumption. The following inequality expresses an energy feasibility condition for a particular sensor:

$$V_{dd}(I_S + I_W)T \le \frac{1}{2}C\left(V_{\text{rec}}^2 - V_{dd}^2\right) \quad (4)$$

i.e., the energy required to read the sensor must not exceed the usable stored energy. This expression can be used to calculate the capacitor size and voltage headroom required to operate a particular sensor, which, in turn, determines the range at which the sensor can be operated.

The current consumptions for the sensor and WISP are I_S and I_W, respectively, C is the capacitance of the storage capacitor, and T is the total time of active operation. The rectified voltage is V_{rec}, and V_{dd} is the required operating voltage. Assuming that the sensor has the same voltage supply as WISP, $V_{dd} = 1.8$ V. The left-hand side of (4) represents the energy consumed by the sensor and WISP during one measurement. The right-hand side represents the usable stored energy above V_{dd}, i.e., the minimum operating voltage of WISP. Inequality (4) makes it clear that the limiting factor when selecting sensors is not only the current consumption (which determines power) but also the total required execution time of the sensor and WISP (energy, rather than power).

V. EXPERIMENTAL RESULTS

Fig. 6 shows the experimental results of WISP performance: rectified output voltage, tag responses per-reader query, and the rate of tag-to-reader packet errors is plotted versus received power (in dBm). The experimental setup consisted of an EPC Gen 1 RFID reader driving a 6-dBi circularly polarized patch antenna. The reader's antenna and WISP were placed 1 m apart and 1 m above the ground to minimize multipath effects. An adjustable attenuator inserted between the reader and its antenna was used to vary the power transmitted to the WISP.

Finally, (2) is used to calculate the path loss over the 1-m separation between WISP and the RFID reader. Thus, the WISP received power is defined as the reader transmit power (1 W), minus the variable attenuator, minus the transmission path loss. It should be noted that the 1-W source represents the peak output power of the RFID reader, whereas the average output power (not considered here) is highly dependent on the reader transmission rate and the specific implantation of the EPC Gen 1 protocol.

To measure the rectified *Output Voltage*, WISP is placed in its low-power state, and the voltage is averaged over a 10-s interval using an oscilloscope. This is necessary to account for the variation in output power as the reader implements the EPC protocol. The resulting plot shows that WISP turns on with a peak received power level of −5.9 dBm, which is significantly more than the average power level of −9.5 dBm measured with

the network analyzer in Fig. 5. To verify that this difference in turn-on threshold is caused by a lower average power in the experimental setup, the RFID reader was replaced with a 915-MHz, 1-W, continuous wave source, and the turn-on power was found to be -8.7 dBm. The 0.8-dBm difference between the continuous source and the network analyzer is thought to be due to the impedance mismatch between the dipole and the analog front end of the WISP, as well as antenna nonidealities. The 2.8-dBm difference between the continuous source and the RFID reader is then due to the lower average power output by the reader.

The plot of tag *Responses per Query* shows the number of successful tag responses received by the reader normalized over the total number of queries made. This is equivalent to the operating duty cycle of the WISP and, as expected, is proportional to the received power. The response rate drops to zero at -7 dB because there is insufficient voltage for operation. At 0-dBm input power, Section IV-B predicted an operational duty cycle of 27% using (3), which is close to the experimental value of 25% from Fig. 6. The reason that the duty cycle (unlike turn-on voltage) is not diminished by the lower average power of the RFID reader is because the duty cycle is normalized to the query rate of the reader. In other words, *Responses per Query* excludes times in which the reader is not transmitting.

The *Uplink Packet Error* represents the percent of query responses made by the tag that is not correctly received by the RFID reader. Due to the limited data interface with the RFID reader selected for the experiment, the number of reader-rejected uplink packets is not directly available. To collect these data, WISP counts the number of query responses it has made and reports the current tally as data encoded in each uplink packet. When the RFID reader application software receives gaps in the running tag response tally, an error is recorded. Fig. 6 shows that as the received power decreases to the point at which sufficient voltage can no longer be rectified for operation, the uplink packet error rate increases. It is theorized that this system instability is due to the brown-out state of MPS430 along with the ring oscillator used as the system clock becoming detuned as the 1.8-V regulator drops out.

VI. Sensors and Applications

Low-power sensors requiring less than 500 μA of current are relatively easy to integrate with WISP. Examples include light, temperature, push buttons, and rectified voltage level. Reference [10] presented the results from a light sensor attached to WISP. The measurement of rectified voltage is easily accomplished with a voltage divider to scale the rectified voltage to the range of 1.8-V ADC. An ultralow-power analog switch can be used to reduce the current drawn between sensor reads.

We found the accuracy and power consumption of the on-chip MSP430 temperature sensor to be disappointing, but more accurate low-power solid-state temperature sensors are readily available, and we added an external temperature sensor to the WISP. Fig. 7 demonstrates the measurement capabilities of WISP over a 70 $^\circ$C temperature range. WISP measurements are sampled from an LM94021 analog temperature sensor, which
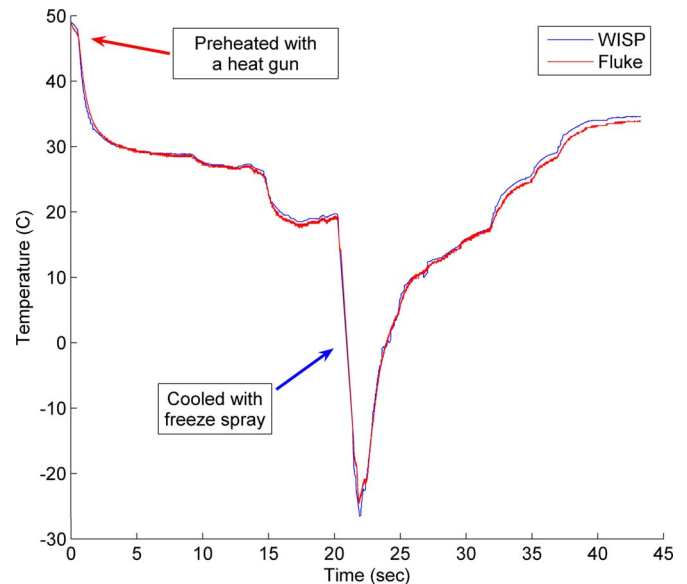

Fig. 7. Cold impulses are applied to WISP and a Fluke multimeter thermal probe and plotted over time.

has 1.8 $^\circ$C accuracy. Using a Fluke thermal probe as a reference, the maximum error recorded between -20 $^\circ$C and 50 $^\circ$C by the WISP was 2 $^\circ$C.

Real-world environmental noise often requires bandlimiting the sensor signal to a few kilohertz or less. Such a filter may have a long time constant. Energy considerations should also be considered from (3) to choose a sufficient capacitor size for the system. For example, powering a 500-μA sensor for 10 ms requires a great deal more energy than RFID communication; a 50-μF capacitor charged to 1.9 V would be needed to provide enough energy to measure the sensor.

A second application of WISP takes advantage of the WISP's computational capabilities. In [11], the authors presented the first implementation of strong encryption (RC5) in a passive UHF RFID tag. Cryptography typically has demanding computational requirements. Previously, it had been standard to assume in the RFID security literature that UHF tags must use "minimalist" cryptosystems with reduced computational requirements, because UHF tags were assumed to support only minimal computational capabilities. We showed in [11] that WISP has enough computational power to implement an ordinary (nonminimalist) cryptosystem: namely RC5.

VII. Conclusion

This paper has presented the design and experimental results for WISP: a battery-free programmable RFID sensor device compliant with the EPC Class 1 Generation 1 protocol. WISP operates from wireless power at a distance of several meters and provides a robust bidirectional communication channel on top of the RFID reader physical layer. Finally, a temperature sensor application is presented as a demonstration of WISP in operation.

VIII. Future Work

Future design efforts will focus on improvements in antenna design, including PCB-integrated antennas, as well as

refinement of the WISP platform to more effectively manage power and increase the operating range of the device. The development of new applications using low-power sensors such as acoustic, pressure, and strain sensors will be investigated. Exploring applications of the onboard computational power, for compression and other embedded sensor data processing functions, is another area for future research. The techniques and lessons learned from the PCB implementation will be transferred to an IC implementation. This will provide lower power consumption and smaller form factor. Finally, new protocols optimized for RFID sensing are an additional area of research suggested by this paper.

REFERENCES

[1] R. Weinstein, "RFID: A technical overview and its application to the enterprise," *IT Prof.*, vol. 7, no. 3, pp. 27–33, May 2005.

[2] D. C. Ranasinghe, K. S. Leong, M. L. Ng, D. W. Engels, and P. H. Cole, "A distributed architecture for a ubiquitous RFID sensing network," in *Proc. Int. Conf. Intell. Sens., Sens. Netw. Inf. Process.*, 2005, pp. 7–12.

[3] M. Philipose, K. P. Fishkin, M. Perkowitz, D. J. Patterson, D. Fox, H. Kautz, and D. Hahnel, "Inferring activities from interactions with objects," *Pervasive Comput.*, vol. 3, no. 4, pp. 50–57, Oct.–Dec. 2004.

[4] R. Want, "Enabling ubiquitous sensing with RFID," *Comput.*, vol. 37, no. 4, pp. 84–86, Apr. 2004.

[5] N. Cho *et al.*, "A 5.1-μW 0.3-mm^2 UHF RFID tag chip integrated with sensors for wireless environmental monitoring," in *Proc. IEEE Eur. Solid State Circuits Conf.*, Grenoble, France, Sep. 2005, pp. 279–282.

[6] F. Kocer and M. P. Flynn, "A new transponder architecture with on-chip ADC for long-range telemetry applications," *IEEE J. Solid-State Circuits*, vol. 41, no. 5, pp. 1142–1148, May 2006.

[7] Microchip Technology Inc., *125 kHz Passive RFID Device With Sensor Input*, Aug. 25, 2005.

[8] M. Philipose, J. R. Smith, B. Jiang, K. Sundara-Rajan, A. Mamishev, and S. Roy, "Battery-free wireless identification and sensing," *Pervasive Comput.*, vol. 4, no. 1, pp. 37–45, Jan. 2005.

[9] J. R. Smith, B. Jiang, S. Roy, M. Philipose, K. Sundara-Rajan, and A. Mamishev, "ID modulation: Embedding sensor data in an RFID timeseries," in *Proc. 7th Inf. Hiding Workshop*, Barcelona, Spain, Jun. 2005, pp. 234–246.

[10] J. R. Smith, A. P. Sample, P. S. Powledge, S. Roy, and A. Mamishev, "A wirelessly-powered platform for sensing and computation," in *Proc. Ubicomp*, 2006, pp. 495–506.

[11] H. Chae, D. Yeager, J. Smith, and K. Fu, "Maximalist cryptography and computation on the WISP UHF RFID tag," in *Proc. Conf. RFID Security*, 2007.

Alanson P. Sample (S'03) received the B.S. degree in electrical engineering in 2005 from the University of Washington (UW), Seattle, where he is currently working toward the M.S. degree in electrical engineering.

He was with the Sensors Energy and Automation Laboratory (SEAL), UW, where he coauthored two papers on autonomous robotic power cable inspection. In 2006, he was a recipient of the Granger Foundation Fellowship. He has interned at Intel Research Seattle three times, from 2005 to 2007, where he published several papers on his work related to RFID and the WISP platform. His interests include RFID, wirelessly powered systems, and embedded systems.

Daniel J. Yeager (S'05) received the B.S. degree (*cum laude*) in electrical engineering in 2006 from the University of Washington, Seattle, where he is currently working toward the M.S. degree in electrical engineering.

In 2007, he was with Intel Research Seattle, where he developed hardware and firmware for wireless battery-free platforms, especially in the realm of UHF RFID. He has authored papers on UHF RFID sensing and encryption and has several patents pending through Intel. His research interests include wireless sensing and energy scavenging.

Pauline S. Powledge received the B.S. degree in computer science from Hunter College, New York, NY, in 1986 and the M.S. degree in computer science from Columbia University, New York, in 1992.

She has previously worked in engineering positions with Internap LLC and WRQ Inc. (now Attachmate Corporation), and was a Member of Technical Staff with AT&T Bell Labs. She is currently a Senior Software Engineer with Intel Research Seattle, Seattle, WA. Her current work is focused on embedded devices, sensors, and low-power wireless networking.

Alexander V. Mamishev (S'92–M'00–SM'06) received the B.S. degree (equivalent certificate) in electrical engineering from Kiev Polytechnic Institute, Kiev, Ukraine, in 1992, the M.S. degree in electrical engineering from Texas A&M University, College Station, in 1994, and the Ph.D. degree in electrical engineering from Massachusetts Institute of Technology, Cambridge, in 1999.

He is currently the Director of the Sensors, Energy, and Automation Laboratory (SEAL), Department of Electrical Engineering, University of Washington, Seattle. He is the author of three book chapters, about 100 journal and conference proceedings, and one patent. His research interests include sensor design and integration, dielectrometry, electric power applications, bioengineering, MEMS, and robotics.

Dr. Mamishev serves as an Associate Editor for the IEEE TRANSACTIONS ON DIELECTRICS AND ELECTRICAL INSULATION. He is the recipient of the National Science Foundation CAREER Award, the IEEE Outstanding Branch Advisor Award, and the University of Washington EE Outstanding Research Advisor Award.

Joshua R. Smith (M'99) received the B.A. degree in computer science and philosophy from Williams College, Williamstown, MA, in 1991, the M.A. degree in physics from the University of Cambridge, Cambridge, U.K., in 1997 (originally the BA Hons. degree in 1993), and the Ph.D. degree from the Massachusetts Institute of Technology, Cambridge, in 1999.

He is currently a Senior Research Scientist with Intel Research Seattle, Seattle, WA, and has affiliate faculty appointments with the University of Washington, Seattle, in both electrical engineering and computer science and engineering. At Intel, he leads the WISP project and the Personal Robotics project. He is an inventor on ten issued U.S. patents. His interests include sensor physics and signal processing; the use of RF signals for sensing, communication, and power transport; and novel sensing techniques for robotic grasping.